Simen Owen Academic Proceedings Series

Vol. 3 2026

Article Open Access

Lift-Drag Characteristics and Vortex Interaction Mechanisms of Two-Dimensional Tandem Airfoils

Dajun Yuan [1,*]

[1] Shandong Experimental High School, Jinan, Shandong, 250001, China
* Correspondence: Dajun Yuan, Shandong Experimental High School, Jinan, Shandong, 250001, China

Abstract: The aerodynamic performance of tandem airfoils arranged in fore-aft configurations has become an important subject in low Reynolds number aerodynamics, owing to its relevance for unmanned aerial vehicles, formation flight, and energy-efficient aircraft. While prior studies have clarified the influence of spacing and positioning on lift and drag, most have focused on time-averaged coefficients or steady conditions, leaving the dynamic relationship between vortex evolution and instantaneous aerodynamic forces insufficiently understood. This study employs large-scale transient numerical simulations to analyze two-dimensional tandem airfoils, with visualization supported by FieldView 20 and quantitative analysis performed in Tecplot. Aerodynamic coefficients, including lift, pressure drag, and viscous drag, were extracted for both fore and aft airfoils, and systematically correlated with transient vortex structures across representative time instants. The results demonstrate that the fore airfoil maintains quasi-steady performance with minimal coefficient fluctuations, serving as a stable aerodynamic baseline. By contrast, the aft airfoil exhibits strong unsteady oscillations in lift and drag, directly governed by vortex growth, detachment, and reattachment, as confirmed by surface pressure distributions and flow field contours. These findings bridge the gap between force production and vortex dynamics in tandem configurations, advancing theoretical understanding of unsteady aerodynamics and offering practical insights for UAV formation design and bio-inspired flight strategies.

Keywords: tandem airfoils; lift-drag characteristics; vortex dynamics; unsteady aerodynamics; low reynolds number

Received: 23 December 2025
Revised: 31 January 2026
Accepted: 10 February 2026
Published: 17 February 2026

1. Introduction

The aerodynamic performance of airfoils remains a central issue in the design and operation of modern aircraft. In particular, the flow characteristics of tandem, or fore-aft arranged, airfoils under low Reynolds number conditions have drawn sustained research attention due to their relevance for unmanned aerial vehicles, formation flight, and energy-efficient aircraft configurations [1]. The lift and drag generated by such configurations are not only critical for stability and maneuverability but also provide a unique opportunity to study the coupling between aerodynamic forces and vortex dynamics. Understanding this coupling is of both theoretical and practical importance, as it may lead to more efficient flight strategies inspired by natural flyers such as birds [2].

Despite significant progress, existing research still presents clear limitations. Classical aerodynamic theories and experimental studies have laid the foundation for understanding lift, drag, and the circulation theorem, but most investigations have focused on single airfoils or simplified steady-state conditions [3]. Early work, such as the experimental studies by Scharpf and Mueller, as well as numerical simulations by Fanjoy and Dorney, has revealed important characteristics of tandem airfoil interactions [4].

Zhang and Yang also conducted experimental investigations under low Reynolds numbers [5]. However, much of this research emphasized either averaged aerodynamic coefficients or restricted flight regimes. As a result, the dynamic correlation between transient vortex evolution and instantaneous aerodynamic forces has not been comprehensively addressed [6]. This gap limits the ability to fully capture the mechanisms underlying lift enhancement, drag variation, and their relation to unsteady vortex structures in tandem configurations.

The objective of this study is therefore to systematically investigate the aerodynamic characteristics of two-dimensional tandem airfoils, with a focus on the correlation between lift-drag performance and vortex dynamics. Specifically, the research seeks to clarify how transient vortex structures influence aerodynamic force production, and how these effects differ between fore and aft airfoils. By identifying these relationships, the study aims to provide both a more complete theoretical framework and practical insights for aerodynamic optimization.

Methodologically, this research employs large-scale aerodynamic simulations to generate detailed transient flow field data. Visualization is conducted through FieldView 20, while Tecplot is used for flow field and force coefficient analysis. Key aerodynamic parameters, lift coefficient, pressure drag coefficient, and viscous drag coefficient, are extracted for both fore and aft airfoils. These data are analyzed in relation to transient vortex structures and pressure distributions across representative time instants. Through this systematic approach, the study builds a direct link between unsteady flow phenomena and aerodynamic force fluctuations.

The academic significance of this work lies in advancing the understanding of unsteady aerodynamic mechanisms in tandem airfoil configurations. By bridging the gap between instantaneous vortex evolution and aerodynamic force generation, the study contributes to the refinement of aerodynamic theory at low Reynolds numbers. The practical significance extends to the design of aircraft and unmanned aerial vehicle formations, where optimizing lift and minimizing drag are essential for endurance and energy efficiency. Furthermore, the findings offer a scientific basis for bio-inspired flight strategies, echoing the efficiency of natural flyers.

The key innovations of this study are reflected in its methodological and analytical approach. By integrating large-scale transient aerodynamic simulations with systematic analyses of force-vortex correlations, this research moves beyond the averaged or steady-state perspectives that dominate earlier studies. It offers a detailed characterization of lift, pressure drag, and viscous drag across multiple typical time instants, thereby elucidating the dynamic mechanisms underlying force production in tandem airfoils. More importantly, it establishes explicit correlations between unsteady vortex structures and aerodynamic force fluctuations in fore-aft arrangements, providing new insights into the mechanisms of aerodynamic interaction. These innovations not only extend theoretical understanding but also provide practical implications for the design and optimization of energy-efficient flight configurations.

2. Literature Review

Research on the aerodynamic characteristics of airfoils has provided a strong foundation for aerodynamics, and tandem airfoils in fore-aft configurations have gained attention for their role in flight efficiency and formation mechanisms. A series of experimental and numerical studies under low Reynolds numbers have confirmed that tandem configurations can significantly alter aerodynamic coefficients compared to isolated single airfoils [7]. These investigations highlight the importance of spacing and relative positioning, showing that tandem arrangements offer advantages for revealing complex aerodynamic interactions.

Despite these advances, limitations remain. Much of the existing work has focused on steady or time-averaged aerodynamic parameters, with limited exploration of unsteady behaviors [8]. While valuable averaged data have been reported, the dynamic coupling between transient vortex evolution and instantaneous aerodynamic forces has not been comprehensively addressed. Some studies expanded understanding of low Reynolds number flow, but many relied on simplified assumptions or were constrained to static regimes [9]. As a result, although the general lift and drag performance of tandem airfoils is documented, the mechanisms by which vortex structures contribute to force variation are still insufficiently explained.

Comparisons across available studies further reveal gaps. Experimental investigations provide reliable results under controlled conditions but often lack the temporal resolution to capture evolving vortex structures [10]. Numerical simulations deliver detailed flow field information but are restricted by computational scale and turbulence modeling assumptions. The divergence between these two approaches underscores the need for methods that integrate transient flow visualization with precise aerodynamic force data [11]. Moreover, prior studies often considered fore or aft airfoils in isolation rather than analyzing their coupled dynamics within a cyclical framework [12].

These shortcomings define a clear research space. The unsteady correlation between aerodynamic loads, lift, pressure drag, and viscous drag, and evolving vortex structures in fore-aft tandem configurations remains insufficiently explored [13]. Few works have systematically mapped aerodynamic coefficients across multiple representative time instants or established a direct force-vortex relationship applicable to both fore and aft airfoils. This lack of integration limits the broader applicability of existing findings to formation flight or energy-efficient aircraft design [14].

The present study responds to these gaps by combining large-scale transient aerodynamic simulations with advanced visualization and analysis tools such as FieldView 20 and Tecplot. By characterizing lift, pressure drag, and viscous drag across representative phases of the flow cycle, it establishes explicit correlations between unsteady vortex structures and aerodynamic forces [15]. In doing so, it advances beyond earlier approaches and contributes a more comprehensive theoretical and practical understanding of tandem airfoil aerodynamics under unsteady conditions.

3. Methodology

3.1. Research Design

This study adopts a computational framework to investigate the aerodynamic characteristics of two-dimensional tandem airfoils. The design is centered on linking transient vortex structures with aerodynamic force production. The methodological framework is divided into three sequential stages:

1) Numerical simulation of fore-aft arranged airfoils under representative flow conditions.
2) Extraction and visualization of transient flow field data, enabling observation of vortex evolution.
3) Correlation analysis between aerodynamic coefficients and vortex dynamics, with particular attention to the fore and aft airfoils.

This workflow is illustrated in Figure 1 (methodology flowchart), showing the closed loop of simulation, data extraction, visualization, and correlation analysis.

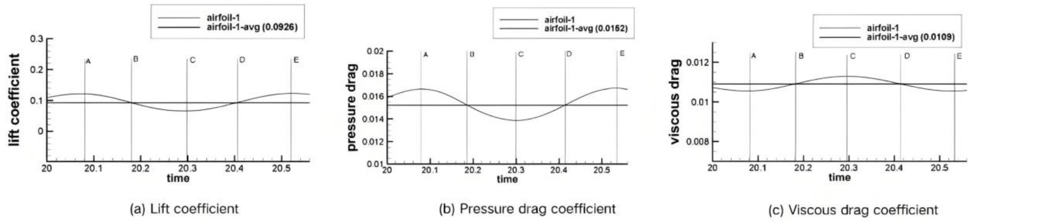

Figure 1. Variations of aerodynamic coefficients of the fore airfoil across one cycle.

3.2. Computational Setup and Tools

3.2.1. Simulation Environment

Large-scale numerical simulations form the basis of this study. Two specialized tools are integrated:

(1) FieldView 20: visualization of instantaneous flow fields, including vortex formation, shedding, and interaction.

(2) Tecplot: post-processing, data extraction, and coefficient-based quantitative analysis.

3.2.2. Data Collection

The following categories of data are systematically collected:

1) Transient flow fields: capturing dynamic vortex evolution across multiple time instants.
2) Integrated aerodynamic coefficients: lift, pressure drag, and viscous drag, obtained for both fore and aft airfoils.

3.3. Aerodynamic Force Coefficients

To quantitatively evaluate the aerodynamic performance of tandem airfoils, three key force coefficients are defined: the lift coefficient, the pressure drag coefficient, and the viscous drag coefficient. These coefficients are normalized by dynamic pressure and reference chord length, ensuring dimensionless comparability across different flow conditions.

3.3.1. Lift Coefficient

The lift coefficient is defined as:

$$C_{py} = \frac{L_{py}}{0.5\rho U_{\infty}^{2} c} = \frac{1}{0.5\rho U_{\infty}^{2} c} \oint_{\Gamma} p\, n_x \, dl \tag{1}$$

where L_{py} is the aerodynamic lift force, ρ is the fluid density, $U\infty$ is the free-stream velocity, c is the chord length, p is the pressure on the airfoil surface, n_x is the unit normal in the x-direction, and Γ denotes the airfoil surface contour.

3.3.2. Pressure Drag Coefficient

The pressure drag coefficient is expressed as:

$$C_{px} = \frac{D_{px}}{0.5\rho U_{\infty}^{2} c} = \frac{1}{0.5\rho U_{\infty}^{2} c} \oint_{\Gamma} p\, n_y \, dl \tag{2}$$

where D_{px} represents the drag force due to surface pressure, and n_y is the unit normal in the y-direction. This coefficient isolates the contribution of pressure differentials to overall drag.

3.3.3. Viscous Drag Coefficient

The viscous drag coefficient is written as:

$$C_{vx} = \frac{D_{vx}}{0.5\rho U_{\infty}^{2} c} = \frac{1}{0.5\rho U_{\infty}^{2} c} \oint_{\Gamma} \tau_w \, t_x \, dl \tag{3}$$

where D_{vx} denotes viscous drag, τ_w is the wall shear stress, and t_x is the tangential vector along the airfoil surface. This coefficient accounts for shear-induced resistance.

3.3.4. Summary of Force Coefficients

Table 1 summarizes the three aerodynamic force coefficients and their physical interpretations.

Table 1. Definitions and physical interpretations of aerodynamic force coefficients.

Coefficient	Formula (integral form)	Physical Meaning
C_{py}	$\frac{1}{0.5\rho U_{\infty}^{2} c}\oint_{\Gamma} p\, n_x\, dl$	Dimensionless lift coefficient
C_{px}	$\frac{1}{0.5\rho U_{\infty}^{2} c}\oint_{\Gamma} p\, n_y\, dl$	Pressure drag coefficient
C_{vx}	$\frac{1}{0.5\rho U_{\infty}^{2} c}\oint_{\Gamma} \tau_w\, t_x\, dl$	Viscous drag coefficient

3.4. Transient Flow Field Analysis

The transient flow fields of both fore and aft airfoils were systematically analyzed to establish direct correlations between aerodynamic forces and vortex structures. For the fore airfoil, the evolution of the wake was observed to determine its influence on downstream unsteadiness. For the aft airfoil, aerodynamic coefficients exhibited strong periodic variations, which were clearly driven by the disturbed inflow generated by the fore airfoil. To capture representative behaviors, five typical instants (A-E) were selected for lift coefficient analysis, seven instants (A-G) for pressure drag, and five instants (A-E) for viscous drag. These instants correspond to critical phases within a flow cycle, such as vortex growth, shedding, and interaction with the airfoil surface. They were subsequently employed to connect transient force fluctuations with detailed flow visualization, forming the foundation for interpreting unsteady aerodynamic mechanisms.

3.5. Visualization and Data Processing

Visualization and data analysis formed an essential component of the methodology. FieldView 20 was utilized to visualize transient flow fields, allowing the identification of vortex formation, separation, and interaction with the airfoil surfaces. Tecplot was employed for quantitative post-processing, extracting aerodynamic coefficients and generating temporal curves that captured periodic variations of lift, pressure drag, and viscous drag. Pressure and vorticity contours were constructed to reveal the spatial development of unsteady structures, while surface pressure distributions at the aft airfoil were obtained for representative instants (A-E). This dual approach of qualitative visualization and quantitative analysis ensured that transient aerodynamic behaviors could be examined from multiple perspectives, providing robust input for subsequent correlation analysis and for the interpretation presented in the results section.

3.6. Correlation Analysis

The correlation analysis was designed to link unsteady vortex dynamics with aerodynamic force fluctuations in a systematic manner. Temporally, the variations of lift, pressure drag, and viscous drag coefficients were compared with the cyclical evolution of vortex shedding, allowing the identification of key phases within each flow cycle. Peaks and troughs in coefficient curves were examined against characteristic instants (A-G) to determine how vortex formation and detachment directly affected aerodynamic performance. Spatially, pressure and vorticity contours were aligned with instantaneous surface pressure distributions to reveal causal mechanisms underlying force production. This dual temporal-spatial approach provided a comprehensive view of how local flow structures influence global aerodynamic forces. In addition, comparative analysis between fore and aft airfoils highlighted the role of upstream wake interference, demonstrating how the fore airfoil modifies downstream flow and amplifies unsteady effects. Together, these analyses established a clear framework for interpreting the dynamic coupling between vortex evolution and aerodynamic loading.

3.7. Technical Route

The technical route of this study followed a structured and reproducible sequence to ensure consistency in both data collection and analysis. The process began with the setup of tandem airfoil geometry and flow conditions, where parameters such as chord length, spacing, and inflow velocity were carefully defined. Transient numerical simulations were then conducted to capture instantaneous flow fields, producing datasets with sufficient temporal resolution to observe vortex formation and shedding. In the third stage, Tecplot was used to extract aerodynamic coefficients, including lift, pressure drag, and viscous drag, while FieldView 20 was applied to visualize flow structures and surface pressure distributions. Finally, these datasets were integrated in a correlation framework that compared force fluctuations with vortex evolution at representative instants (A-G). This sequential approach not only ensured reliability and transparency but also provided a clear methodological foundation for interpreting unsteady aerodynamic mechanisms in tandem airfoil configurations.

3.8. Reliability and Validity

Ensuring the reliability and validity of the methodology was an integral part of the study. Reliability was achieved by conducting repeated simulations under identical flow conditions and geometric parameters, which confirmed the stability and reproducibility of the aerodynamic coefficients and flow structures obtained. Cross-validation between FieldView 20 and Tecplot further enhanced confidence, as visualization and quantitative analysis yielded consistent trends in vortex evolution and aerodynamic force variation. Validity was addressed through the careful selection of representative instants (A-G), which captured the essential unsteady features of the flow cycle, including vortex growth, shedding, and reattachment. By focusing on both instantaneous and time-averaged results, the analysis avoided bias toward either steady or transient interpretations. Together, these measures provided a rigorous methodological foundation, ensuring that the subsequent results and conclusions were both credible and broadly applicable to tandem airfoil studies.

3.9. Summary

In summary, the methodology integrates numerical simulation, coefficient analysis, and flow visualization into a coherent framework. The adoption of representative time instants ensures that both transient and averaged behaviors are systematically captured. The combination of FieldView 20 and Tecplot provides robust support for subsequent analysis, laying the foundation for a comprehensive results section.

4. Results and Analysis

4.1. Fore Airfoil Aerodynamic Characteristics

The aerodynamic performance of the fore airfoil demonstrates a quasi-steady pattern across the investigated cycle. As shown in Figure 1, the three key aerodynamic coefficients, lift (Figure 1(a)), pressure drag (Figure 2(b)), and viscous drag (Figure 1(c)), exhibit only minor oscillations over the five representative instants (A-E). The lift coefficient fluctuates around an average value close to 0.09, while the amplitudes of pressure drag (≈0.015) and viscous drag (≈0.011) remain similarly small. This stability indicates that the aerodynamic loads on the fore airfoil are weakly influenced by unsteady wake phenomena.

At instant A, the lift coefficient corresponds to a fully attached flow condition, with balanced circulation and minimal disturbance near the trailing edge. Between instants B and C, the lift curve shows a slight reduction, associated with the onset of weak downstream wake development. However, the corresponding drag coefficients remain nearly unchanged, reflecting that the boundary layer is largely stable. At instant D, small oscillations appear, but the magnitudes are insufficient to affect the overall aerodynamic balance. By instant E, the flow reattaches and the coefficients return close to their mean values, completing the quasi-periodic cycle.

The combination of low-amplitude oscillations and consistent mean values across all coefficients demonstrates that the fore airfoil contributes primarily steady lift production and stable drag characteristics. Unlike the aft airfoil, which is subjected to significant unsteady disturbances from wake impingement, the fore airfoil operates under circulation-dominated mechanisms with minimal vortex shedding influence. This finding highlights the asymmetry of tandem configurations: the fore airfoil provides a predictable aerodynamic baseline, against which the strongly unsteady aft airfoil dynamics can be interpreted.

4.2. Aft Airfoil Aerodynamic Characteristics

In contrast to the fore airfoil, the aft airfoil exhibits strongly unsteady aerodynamic behavior, which is directly attributable to the wake interference generated upstream. As shown in Figure 2, all three aerodynamic coefficients display clear periodic oscillations within one flow cycle, reflecting the dominant influence of transient vortex interactions.

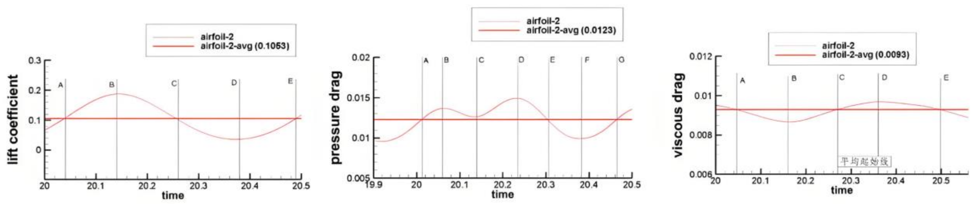

(a) Lift coefficient (b) Pressure drag coefficient (c) Viscous drag coefficient

Figure 2. Variations of aerodynamic coefficients of the aft airfoil across one cycle.

The lift coefficient (Figure 2(a)) fluctuates significantly around its mean value. At instant A, the lift begins to rise as a coherent vortex approaches the leading edge, generating additional suction on the upper surface. By instant B, the coefficient reaches a local peak, indicating maximum lift enhancement due to strong vortex-induced circulation. Subsequently, at instant C, the vortex detaches and convects downstream, producing a sharp decrease in lift. The coefficient partially recovers at instants D and E, but the oscillatory nature remains evident. This cyclic rise-and-fall behavior contrasts sharply with the quasi-steady lift of the fore airfoil and confirms that the aft element is governed by unsteady vortex shedding.

The pressure drag coefficient (Figure 2(b)) demonstrates an even more pronounced periodicity, captured across seven representative instants (A-G). Local maxima correspond to phases of intensified adverse pressure gradients induced by vortex impingement, while minima coincide with periods of flow reattachment and reduced pressure difference between upper and lower surfaces. The pressure drag curve underscores the high sensitivity of the aft airfoil to instantaneous wake structures, with variations substantially larger than those observed for the fore element.

The viscous drag coefficient (Figure 2(c)) shows more moderate but still noticeable oscillations across the five instants (A-E). Increases in viscous drag correspond to periods of boundary-layer thickening and localized separation, particularly when vortices interact with the trailing edge. Conversely, decreases occur during partial reattachment, when wall shear stress is reduced. Although the amplitude of viscous drag fluctuations is smaller than that of lift or pressure drag, its cyclical character highlights the role of boundary-layer dynamics in shaping overall aerodynamic resistance.

Taken together, these results confirm that the aft airfoil operates under strongly unsteady conditions, in sharp contrast to the quasi-steady performance of the fore airfoil. The lift, pressure drag, and viscous drag are all modulated by periodic vortex interactions, demonstrating that downstream elements in tandem configurations are inherently governed by transient aerodynamic mechanisms.

4.3. Pressure Distribution and Flow Structures of the Aft Airfoil

To further reveal the mechanisms driving unsteady aerodynamic coefficients, the instantaneous surface pressure distributions and flow field contours of the aft airfoil were analyzed at five representative instants (A-E). As shown in Figure 3, the pressure fields and vortex structures exhibit a strong correlation with the cyclic variations of lift and drag coefficients described in Section 4.2.

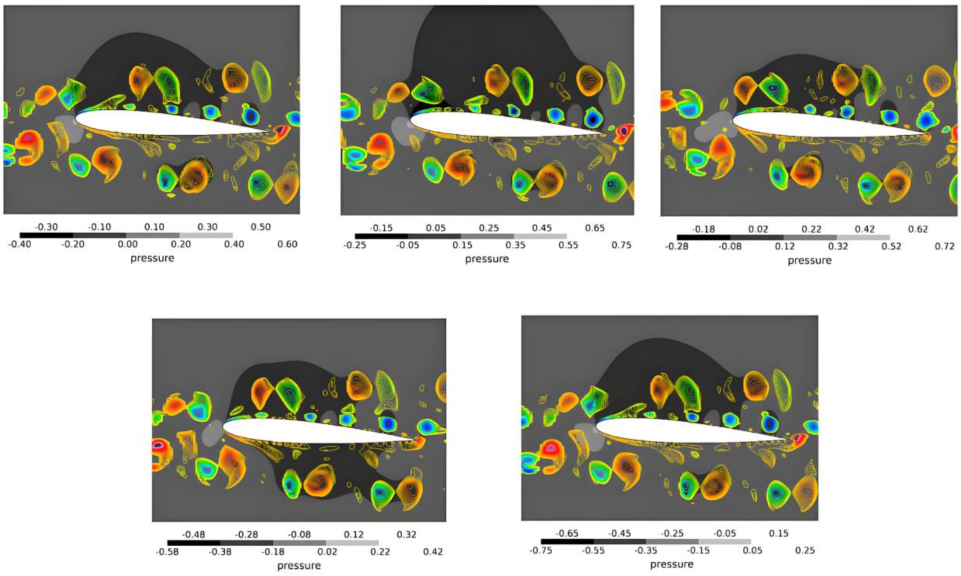

Figure 3. Surface pressure distributions and flow field contours of the aft airfoil at representative instants (A-E).

At instant A, the flow over the aft airfoil remains largely attached. The suction peak is moderate and distributed smoothly along the upper surface, corresponding to the initial rise of the lift coefficient. By instant B, a coherent vortex begins to form near the trailing edge, creating localized low-pressure regions on the suction surface. This leads to an increase in lift and a simultaneous rise in pressure drag.

At instant C, the vortex detaches and convects downstream, breaking the favorable pressure gradient. This redistribution weakens the suction on the upper surface and reduces lift, while the trailing-edge separation increases viscous effects. The consequence is a marked dip in both lift and drag coefficients, consistent with the trends observed in Figure 2.

At instant D, strong vortex impingement on the suction surface produces concentrated low-pressure zones and enhanced adverse pressure gradients. This interaction sharply amplifies the oscillations in aerodynamic forces, resulting in a local maximum in drag and secondary peaks in lift. Finally, at instant E, the flow shows signs of reattachment, with the suction distribution partially recovering and the aerodynamic coefficients returning toward their mean values, completing the unsteady cycle.

These observations confirm that the aft airfoil's aerodynamic behavior is governed not by steady circulation, but by successive phases of vortex growth, detachment, and reattachment. The pressure contour evolution directly explains the cyclic oscillations in lift and drag coefficients, highlighting that unsteady vortex dynamics are the dominant mechanism shaping aerodynamic performance in tandem configurations.

Visualization results showing the evolution of surface pressure and iso-contour fields, illustrating the direct correlation between vortex dynamics and fluctuations in aerodynamic force coefficients.

4.4. Mechanisms of Lift and Drag

The comparison between fore and aft airfoils highlights the asymmetric mechanisms of force generation in tandem configurations, reflecting the dual contributions of quasi-steady upstream circulation and unsteady downstream vortex interactions.

For the fore airfoil, lift is generated primarily by steady circulation around the chord, while drag is dominated by viscous shear along the surface. As shown in Figure 1, the small amplitude of oscillations in lift, pressure drag, and viscous drag coefficients confirms that the fore element operates under near-steady conditions. Vortex shedding in its wake has limited feedback on its own surface loading, resulting in predictable and stable aerodynamic forces.

For the aft airfoil, however, unsteady mechanisms dominate. The coefficient curves in Figure 2 reveal that lift enhancement occurs when vortices impinge on the suction surface, intensifying low-pressure regions and strengthening circulation. Conversely, lift reduction coincides with vortex detachment and downstream convection. Pressure drag exhibits strong oscillations in response to alternating high- and low-pressure regions generated by successive vortex interactions, while viscous drag fluctuates with boundary-layer separation and reattachment, as confirmed by the pressure contour visualizations in Figure 3. These transient processes act in phase with vortex dynamics, directly driving the cyclical variations observed in the aerodynamic coefficients.

This asymmetry demonstrates that tandem configurations inherently combine quasi-steady upstream performance with strongly unsteady downstream dynamics. The fore airfoil provides a stable reference load, while the aft airfoil captures the full influence of vortex growth, detachment, and reattachment. Together, these findings emphasize the critical role of vortex-force coupling in tandem systems, explaining both the aerodynamic benefits and the challenges of unsteady load management in multi-element configurations.

5. Discussion and Conclusion

The results of this study reveal a clear asymmetry in aerodynamic mechanisms between the fore and aft airfoils in tandem configurations. The fore airfoil exhibits quasi-steady behavior, with lift and drag primarily governed by circulation and viscous shear, and only minor oscillations observed. In contrast, the aft airfoil shows pronounced unsteady fluctuations in all aerodynamic coefficients, directly linked to vortex evolution, detachment, and reattachment. This pattern demonstrates that wake interference transforms the aft airfoil into a vortex-dominated system, where transient structures, rather than steady circulation, govern force production. Such findings underscore the essential role of vortex-force coupling in multi-element aerodynamics.

When compared with prior literature, these results align with earlier observations that tandem arrangements amplify unsteady aerodynamic effects. However, unlike studies that emphasized averaged aerodynamic coefficients, the present work establishes a direct correlation between instantaneous vortex evolution and coefficient fluctuations. In doing so, it provides a more complete explanation of the mechanisms underlying lift enhancement and drag variability. This work therefore extends the insights of Scharpf and Mueller, who highlighted low-Reynolds-number effects, by demonstrating how temporal resolution of vortex dynamics is critical for accurate characterization of tandem airfoil performance.

Despite these contributions, certain limitations must be acknowledged. The simulations were restricted to two-dimensional configurations, which inevitably neglect spanwise effects and three-dimensional instabilities that may arise in realistic flows. Additionally, the selected Reynolds number and geometric spacing parameters, though representative, limit the generalizability of the results across broader aerodynamic conditions. The reliance on numerical simulations, even with validation through established software tools, also introduces uncertainties tied to turbulence modeling and grid resolution.

Future research should therefore expand toward three-dimensional tandem configurations, incorporating a wider range of Reynolds numbers and spacing ratios to assess robustness under more practical flight regimes. Moreover, coupling high-fidelity simulations with experimental flow visualization would further validate the vortex-force correlations observed here. Beyond academic insights, these findings offer practical implications for formation flight, UAV swarm design, and bio-inspired configurations, where understanding and managing unsteady aerodynamic interactions are essential for achieving efficiency and stability.

References

1. D. Azad, A. Sunny Kumar, V. Ramana Menda, P. K. Swain, S. Vadapalli, and D. Bommana, "The impact of flapping trajectories on the induced thrust of a Single and tandem configuration flapping foil," *Journal of Offshore Mechanics and Arctic Engineering*, vol. 146, no. 5, p. 051301, 2024. doi: 10.1115/1.4064500
2. D. Ma, B. Song, S. Gao, D. Xue, and J. Xuan, "Designing efficient bird-like flapping-wing aerial vehicles: insights from aviation perspective," *Bioinspiration & Biomimetics*, vol. 19, no. 6, p. 061001, 2024. doi: 10.1088/1748-3190/ad88c4
3. D. F. Scharpf, and T. J. Mueller, "Experimental study of a low Reynolds number tandem airfoil configuration," *Journal of aircraft*, vol. 29, no. 2, pp. 231-236, 1992. doi: 10.2514/3.46149
4. D. W. Fanjoy, and D. J. Dorney, "Numerical simulations of tandem-airfoil aerodynamics (No. 961295)," *SAE Technical Paper*, 1996.
5. G. Q. Zhang, and S. X. Yang, "Experimental investigation of the aerodynamic characteristics of tandem-airfoil based on low Reynolds number," *Jisuan Lixue Xuebao/Chinese Journal of Computational Mechanics*, vol. 27, no. 4, pp. 733-737, 2010.
6. H. Lee, B. Sengupta, M. S. Araghizadeh, and R. S. Myong, "Review of vortex methods for rotor aerodynamics and wake dynamics," *Advances in Aerodynamics*, vol. 4, no. 1, p. 20, 2022. doi: 10.1186/s42774-022-00111-3
7. Q. Zhang, R. Xue, and H. Li, "Aerodynamic exploration for tandem wings with smooth or corrugated surfaces at low Reynolds number," *Aerospace*, vol. 10, no. 5, p. 427, 2023. doi: 10.3390/aerospace10050427
8. H. Zhi, T. Xiao, N. Qin, S. Deng, and Z. Lu, "On-the-Fly Unsteady Adjoint Aerodynamic and Aeroacoustic Optimization Method," *AIAA Journal*, vol. 62, no. 12, pp. 4779-4797, 2024. doi: 10.2514/1.j064455
9. O. Pomerenk, and L. Ristroph, "Aerodynamic equilibria and flight stability of plates at intermediate Reynolds numbers," *arXiv preprint arXiv:2408.08864*, 2024. doi: 10.1017/jfm.2025.10275
10. F. Beaumont, S. Murer, F. Bogard, and G. Polidori, "The aerodynamic mechanisms of the formation flight of migratory birds: A narrative review," *Applied Sciences*, vol. 14, no. 13, p. 5402, 2024. doi: 10.3390/app14135402
11. M. Ge, G. Zhang, and X. Zhang, "Recent Developments and Future Directions in Flow Visualization: Experiments and Techniques," *Fluids*, vol. 10, no. 2, p. 23, 2025. doi: 10.3390/fluids10020023
12. K. S. Priyanka, J. M. L. Jeyan, and R. S. Vihar, "A Review on a Reassess Swot up on Airfoil Stall and Flow Separation Delay for a Range of Limitations Associated with Aerodynamics and Wing Profile," *International Journal of Advanced Science and Technology*, vol. 29, no. 06, pp. 7659-7668, 2020.
13. F. Jafari, D. Holden, R. LaFoy, P. P. Vlachos, and J. J. Socha, "The aerodynamics of flying snake airfoils in tandem configuration," *Journal of Experimental Biology*, vol. 224, no. 14, p. jeb233635, 2021. doi: 10.1242/jeb.233635
14. F. Beaumont, S. Murer, F. Bogard, and G. Polidori, "Aerodynamic mechanisms behind energy efficiency in migratory bird formations," *Physics of Fluids*, vol. 37, no. 2, 2025. doi: 10.1063/5.0252553
15. M. Graham, and J. Li, "Vortex shedding and induced forces in unsteady flow," *The Aeronautical Journal*, pp. 1-42, 2024.